

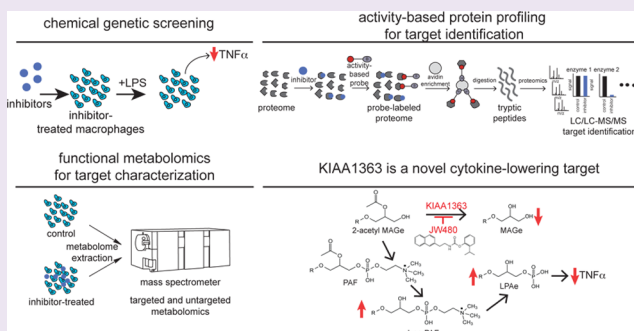
Chemical Genetics Screening Reveals KIAA1363 as a Cytokine-Lowering Target

Devon M. Hunerdosse, Patrick J. Morris, David K. Miyamoto, Karl J. Fisher, Leslie A. Bateman, Jonathan R. Ghazaleh, Sharon Zhong, and Daniel K. Nomura*

Program in Metabolic Biology, University of California, Berkeley, Berkeley, California 94720, United States

Supporting Information

ABSTRACT: Inflammation is a hallmark of many human diseases, including pain, arthritis, atherosclerosis, obesity and diabetes, cancer, and neurodegenerative diseases. Although there are several successfully marketed small molecules anti-inflammatory drugs such as cyclooxygenase inhibitors and glucocorticoids, many of these compounds are also associated with various adverse cardiovascular or immunosuppressive side effects. Thus, identifying novel anti-inflammatory small molecules and their targets is critical for developing safer and more effective next-generation treatment strategies for inflammatory diseases. Here, we have conducted a chemical genetics screen to identify small molecules that suppress the release of the inflammatory cytokine $\text{TNF}\alpha$ from stimulated macrophages. We have used an enzyme class-directed chemical library for our screening efforts to facilitate subsequent target identification using activity-based protein profiling (ABPP). Using this strategy, we have found that KIAA1363 is a novel target for lowering key pro-inflammatory cytokines through affecting key ether lipid metabolism pathways. Our study highlights the application of combining chemical genetics with chemoproteomic and metabolomic approaches toward identifying and characterizing anti-inflammatory small molecules and their targets.



Inflammation is normal defense mechanism against infection or tissue injury. However, chronic or nonresolving inflammation can lead to a wide range of pathologies including cancer, neurodegenerative diseases, and diabetes.^{1–4} Many biochemical pathways have been implicated in driving or suppressing the inflammatory response. Examples include pro-inflammatory prostaglandins and anti-inflammatory resolvins, glucocorticoids, and endocannabinoid signaling molecules.^{5–8} These metabolites are controlled by their biosynthesizing and degrading enzymes, and exerting control over these biochemical pathways holds great promise for the treatment of inflammation and associated complex diseases. A prominent example is the nonsteroidal anti-inflammatory drugs (NSAIDs) (e.g., aspirin and ibuprofen) that target cyclooxygenases (COXs) and are clinically used for pain, inflammation, and arthritis but have been shown in mouse models to be protective against neurodegenerative diseases, diabetes, and cancer.^{2,9–13} However, many of these agents also show negative effects that prevent long-term usage that would be necessary for these complex diseases (e.g., cardiovascular or gastrointestinal side effects with COX inhibitors).¹³ It is therefore critical to gain a deeper understanding into the metabolic pathways that underlie inflammation.

Chemical genetics represents a powerful approach toward discovery of novel and effective small molecules for treatment of complex diseases.¹⁴ Unlike the traditional, target-based screen that relies on a predefined, sometimes poorly validated

target, a chemical genetics-based phenotypic screen efficiently interrogates entire metabolic or molecular signaling pathways in an unbiased manner for the most drug-sensitive node. However, the single most significant impediment associated with this approach is the identification of the targets of the most efficacious small molecules.¹⁴ To address this challenge, we have combined a chemical genetic screen for identifying pro-inflammatory cytokine-lowering small molecules with chemoproteomic and metabolomic platforms to enable straightforward identification of lead compounds, their targets, and their mechanisms.

Here, we performed a chemical genetics screen using a serine hydrolase-directed inhibitor library in macrophages to discover new anti-inflammatory small molecules. We coupled this with a functional chemoproteomics platform to identify their biological targets and used metabolomic approaches to characterize the mechanism of anti-inflammatory action. Using this pipeline, we have identified that the serine hydrolase KIAA1363 is a novel anti-inflammatory target and that KIAA1363-selective inhibitors lower key pro-inflammatory cytokines through modulating ether lipid signaling pathways.

Received: September 8, 2014

Accepted: October 24, 2014

Published: October 24, 2014

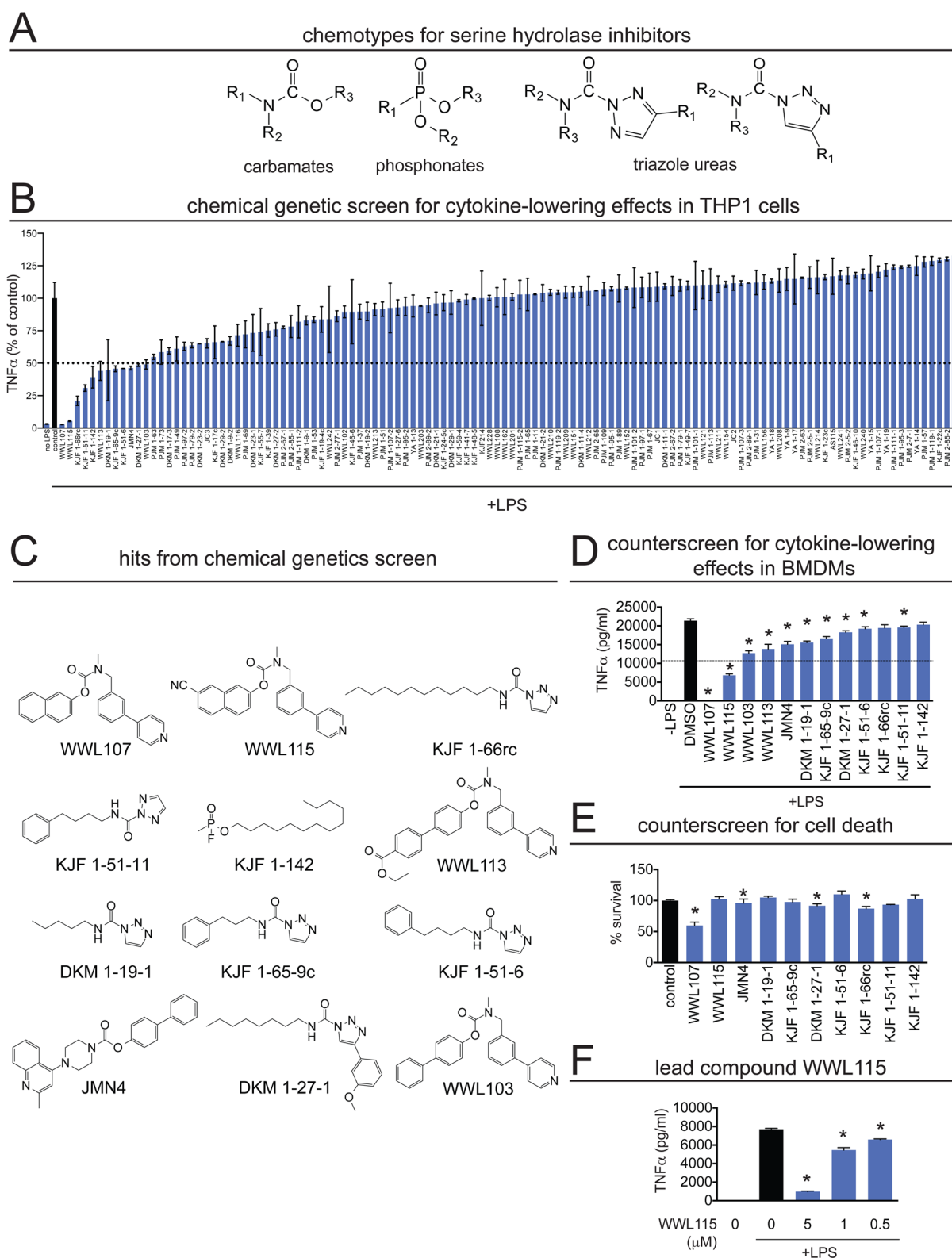


Figure 1. Chemical genetics screening of a serine hydrolase-directed small molecule library reveals new candidate anti-inflammatory small molecules. (A) We screened a library of small molecules based on known serine hydrolase inhibitor scaffolds: carbamates, phosphonates, and triazole ureas. R groups represent diversification points on the small molecules. (B) We screened 120 compounds for agents that lower LPS-induced TNF α secretion from THP1 monocytes. THP1 cells were pretreated with each inhibitor (5 μ M) in serum-free RPMI for 1 h before stimulating with LPS (2 μ g/mL) for 6 h. TNF α levels in media were then assayed by ELISA. Data are displayed as a percent of vehicle-treated, LPS-stimulated controls. (C) Shown are structures of the 12 small molecules that decreased LPS-stimulated TNF α secretion by greater than 50%. (D) We next counterscreened the top 12 compounds to identify agents that also lowered TNF α in primary mouse bone marrow-derived macrophages (BMDMs). BMDMs were preincubated with inhibitor (5 μ M) in serum-free DMEM for 1 h before stimulating with LPS (100 ng/mL) for 6 h. The conditioned medium was assayed for TNF α levels by ELISA. (E) We also counterscreened the lead compounds for cytotoxic agents by performing a cell survival assay using

Figure 1. continued

Hoescht staining. Data are presented as a percent of vehicle-treated cells. (F) WWL115 is the only compound that significantly lowers LPS-stimulated TNF α by greater than 50% in BMDMs without causing cytotoxicity. We show dose-dependent reductions in LPS-induced TNF α secretion with WWL115 treatment in BMDMs. Bar graphs in panels B and D–F are presented as mean \pm SEM. Data represent $n = 2$ /group for panel B and $n = 3$ /group per group for panels D–F. Significance is presented as $*p < 0.05$, comparing inhibitor treated groups to vehicle-treated, LPS-stimulated controls.

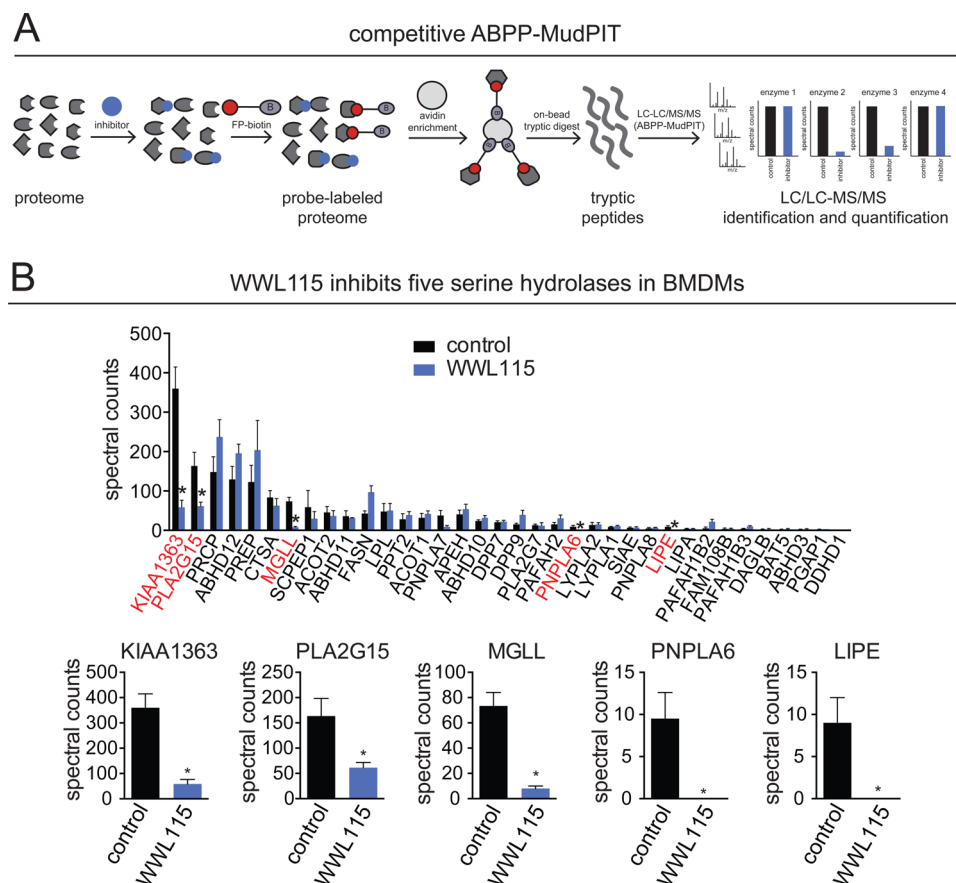


Figure 2. ABPP analysis of WWL115 reveals five serine hydrolase targets involved in lipid metabolism. (A) Competitive ABPP workflow for WWL115 target discovery. BMDMs were treated *in situ* with vehicle (DMSO) or WWL115 (5 μ M), after which BMDM lysates were labeled with the serine hydrolase activity-based probe FP-biotin followed by avidin enrichment, trypsinization, and analysis of serine hydrolase activities by LC–LC–MS/MS (MudPIT) (ABPP-MudPIT). (B) ABPP-MudPIT profiling of WWL115-treated BMDMs reveals five significantly inhibited serine hydrolases. Data are presented as mean \pm SEM; $n = 3$ –4/group. Significance is presented as $*p < 0.05$ between inhibitor and control-treated groups.

RESULTS AND DISCUSSION

Chemical Genetics Screen for Serine Hydrolase Inhibitors that Lower TNF α Release in Macrophages Reveals a Lead Anti-Inflammatory Compound. For our chemical genetics screening strategy, we chose to focus on a small molecule library directed toward the serine hydrolase superfamily, because several members of this enzyme class have previously been implicated in inflammation, including PLA2G4A, MGLL, and PLA2G7.¹⁵ Serine hydrolases make up a large class of metabolic enzymes, which include lipases, esterases, hydrolases, proteases, and peptidases, that serve vital (patho)physiological functions in numerous biological processes.¹⁵ Previous studies have shown that the carbamate, phosphonate, and triazole urea chemotypes are optimal for covalent inhibition of serine hydrolases (Figure 1A).^{16–18} With diversification of substituents, many studies have shown that selectivity can be attained for specific members of the serine hydrolase class.^{16–20}

We screened a library of 120 compounds to identify small molecules that inhibited lipopolysaccharide (LPS)-induced tumor necrosis factor- α (TNF α) secretion from the THP1 human monocyte cell line (Figure 1B and Supporting Information Table 1). This compound library consisted of carbamates, phosphonates, and triazole ureas obtained from the Cravatt and Casida laboratories from previous studies as well as several newly synthesized compounds.^{17,18,21–23} Among the compounds tested, we identified 12 inhibitors that lowered LPS-induced TNF α secretion in THP1 cells by >50% (Figure 1B,C). Although we used THP1 cells for our initial screening efforts, this cell line may not be representative of primary macrophages. We thus performed a counterscreen to identify those inhibitors that also lowered LPS-induced TNF α secretion from primary mouse bone marrow-derived macrophages (BMDMs). Although most of the 12 initial leads significantly lowered TNF α levels, only two of the compounds showed >50% decreases in LPS-stimulated TNF α secretion in this cell type: WWL107 and WWL115 (Figure 1D). To eliminate any

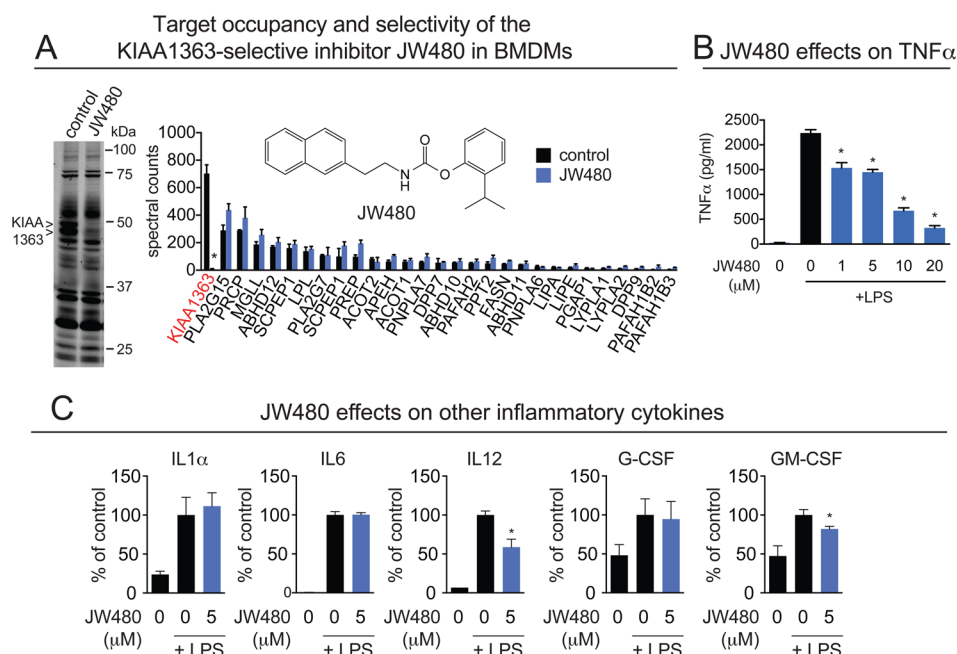


Figure 3. KIAA1363-selective inhibitor JW480 recapitulates the TNF α -lowering effects of WWL115. (A) Gel-based ABPP and ABPP-MudPIT analysis confirm both *in situ* occupancy and selectivity of JW480 as a KIAA1363 inhibitor in BMDMs. (B) JW480 lowers LPS-induced TNF α secretion in a dose-dependent manner. (C) Effect of JW480 on other inflammatory cytokine levels in BMDMs. For experiments in panels A–C, BMDMs were preincubated for 1 h with JW480 at the indicated concentrations. After stimulation with LPS (100 ng/mL) for 6 h, cells were harvested for ABPP analysis, and media was analyzed for secreted TNF α levels by ELISA. Data are presented as mean \pm SEM; $n = 3$ –4/group. Significance is presented as $*p < 0.05$, comparing inhibitor-treated groups to vehicle-treated, LPS-stimulated controls.

compounds that may be lowering TNF α due to cytotoxicity, we also performed a cell survival counterscreen and found that WWL107 significantly impaired cell viability, leaving WWL115 as our lead compound for further study (Figure 1E). We show that WWL115 lowers LPS-induced TNF α release in BMDMs in a dose-dependent manner (Figure 1F).

Chemoproteomic Analysis of WWL115 Reveals Five Significantly Inhibited Serine Hydrolases. Our chemical genetics screen in both THP1 and BMDMs revealed WWL115 as a promising lead anti-inflammatory compound. We next wanted to identify the targets of WWL115 in BMDMs to determine the serine hydrolase(s) responsible for its inflammatory cytokine-lowering effects. To achieve this, we used a chemoproteomic strategy termed activity-based protein profiling (ABPP), a technology that uses active site-directed chemical probes to directly assess the activities of large numbers of enzymes in complex proteomes.^{24–26} Small molecule inhibitors can be competed against activity-based probe binding to enzymes, thus enabling identification of functionally inhibited targets of lead compounds that arise from chemical genetic screens (Figure 2A).^{25,27,28} Here, we used a competitive ABPP platform using the serine hydrolase activity-based probe, fluorophosphonate-biotin (FP-biotin), to identify the serine hydrolase targets inhibited *in situ* in BMDMs by WWL115. We treated BMDMs with vehicle or WWL115 and subsequently labeled cell lysates with FP-biotin, followed by avidin-enrichment, trypsinization, and analysis of tryptic peptides by multidimensional protein identification technology (ABPP-MudPIT). Inhibited targets manifested as loss of spectral counts compared with vehicle treatment. Among the 36 serine hydrolases enriched by our activity-based probe, we found 5 lipases that were significantly inhibited by WWL115: KIAA1363, PLA2G15, MGLL, PNPLA6, and LIPE (Figure 2B).

Characterizing KIAA1363 as a Novel Anti-Cytokine Target in BMDMs. Among the 5 targets identified for WWL115, KIAA1363 was the most abundant serine hydrolase in BMDMs. Chang et al. recently developed a highly selective KIAA1363 inhibitor JW480 that irreversibly inhibited this enzyme both *in situ* in cancer cells and *in vivo* in mice.¹⁹ To confirm target occupancy and selectivity of this inhibitor in macrophages, we treated BMDMs with JW480 and assessed the selectivity of this inhibitor by competitive ABPP using both FP-rhodamine and FP-biotin for gel-based fluorescence and ABPP-MudPIT analysis, respectively. We confirmed that JW480 was highly selective in BMDMs and inhibited only KIAA1363 among all detectable serine hydrolase activities (Figure 3A).

We next tested whether JW480 could recapitulate the TNF α -lowering effects of WWL115. We find that JW480 significantly lowers LPS-induced TNF α secretion from BMDMs in a dose-responsive manner to levels comparable to those observed with WWL115, indicating that KIAA1363 was largely responsible for the TNF α -lowering effects of this compound. We also show that KIAA1363 inhibition by JW480 selectively impairs certain inflammatory cytokines in addition to TNF α , including interleukin-12 (IL12) and granulocyte macrophage colony-stimulating factor (GM-CSF), without affecting other inflammatory cytokines such as IL1 α , IL6, and granulocyte stimulating factor (G-CSF). We also tested the contribution of MGLL using the selective MGLL inhibitor JZL184 because MGLL inhibitors have been shown to elicit anti-inflammatory effects in specific paradigms. We find that MGLL inhibition by JZL184 has no effect in lowering LPS-induced TNF α secretion in BMDMs (Supporting Information Figure 1).

While we show here that KIAA1363 inhibition is a unique and novel strategy for lowering key LPS-induced pro-inflammatory cytokine levels, we cannot rule out the contribution of the remaining three targets, PLA2G15,

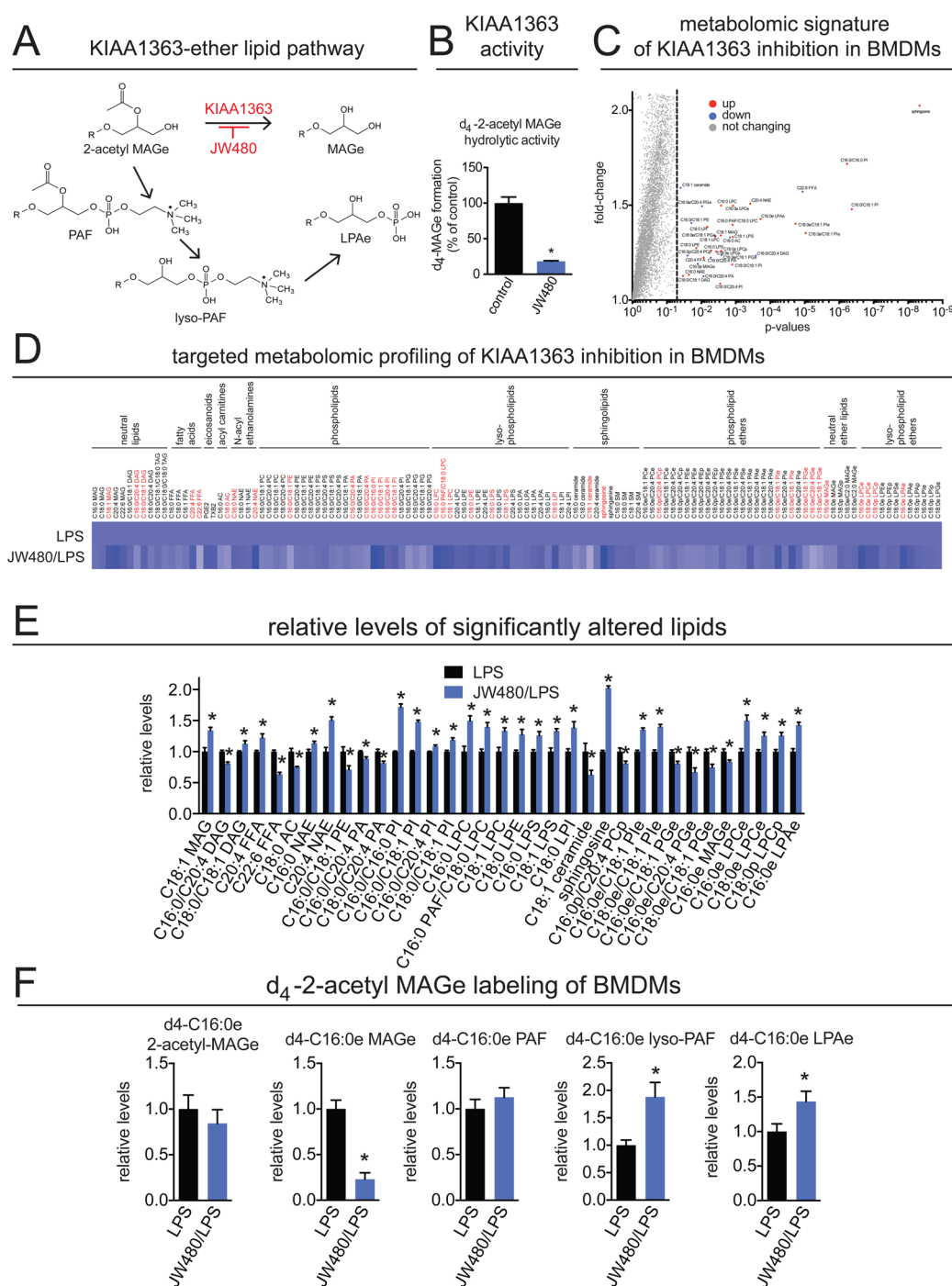


Figure 4. Lipidomic profiling reveals an ether lipid network regulated by KIAA1363 in BMDMs. (A) KIAA1363 is thought to control the formation of monoalkylglycerol ether (MAGe) from the hydrolysis of 2-acetyl MAGe, the penultimate precursor in the biosynthesis of platelet-activating factor (PAF). (B) KIAA1363 activity, assessed by measuring *d*₄-2-acetyl MAGe hydrolysis, is significantly inhibited in JW480-treated BMDMs (5 μ M, 4 h). (C–E) Targeted and untargeted metabolomic analysis of the nonpolar metabolome of JW480-treated BMDMs reveals alterations in the levels of 35 lipid species, shown as a volcano plot in (C) with all ions detected, shown as a heatmap in (D) that includes all targeted lipidomic data by lipid class, and shown in (E) by only the lipids that were significantly altered by JW480 treatment. (F) *d*₄-2-Acetyl MAGe isotopic incorporation into ether lipid metabolites in the KIAA1363 pathway. BMDMs were preincubated with JW480 (5 μ M) or vehicle for 1 h before adding LPS (100 ng/mL) and *d*₄-2-acetyl MAGe (10 μ M) for 15 min. Isotopic incorporation into ether lipid metabolites was analyzed by LC–MS/MS. Data are presented as mean \pm SEM; *n* = 4–5/group. Significance is presented as **p* < 0.05, comparing inhibitor-treated groups to vehicle-treated, LPS-stimulated controls, except in panel B, where cells were not treated with LPS.

PNPLA6, and LIPE. We attempted to knockdown the expression of these enzymes using RNA interference approaches, but we could not achieve sufficient knockdown in BMDMs, and there are a lack of selective pharmacological tools for interrogating the remaining enzymes (data not

shown). Nonetheless, LIPE (hormone-sensitive lipase) blockade has been linked to sterility, and PNPLA6 (also known as neuropathy target esterase) blockade causes peripheral neuropathy and demyelination, thus precluding these enzymes as potential therapeutic targets.^{29,30} PLA2G15 may be of interest

since other phospholipase A2 enzymes have been shown to be anti-inflammatory targets.

Metabolomic Profiling Reveals Key Anti-Inflammatory Lipids Regulated by KIAA1363 in BMDMs. We next used untargeted and targeted liquid chromatography–mass spectrometry (LC–MS)-based metabolomic platforms to investigate the mechanism through which KIAA1363 blockade lowered LPS-induced TNF α release from BMDMs. KIAA1363 was previously characterized as a serine hydrolase that deacetylates the ether lipid 2-acetyl monoalkylglycerol ether (2-acetyl-MAGe or C16:0e/C2:0 MAGe), the penultimate precursor in the *de novo* biosynthesis of platelet activating factor (PAF), to the product monoalkylglycerol ether (MAGe) (Figure 4A).^{31,32} Consistent with its role, we show that *in situ* treatment of BMDMs with JW480 inhibits *d*₄-2-acetyl-MAGe hydrolytic activity in BMDMs (Figure 4B).

Since KIAA1363 is a deacetylase of an ether lipid, we focused our metabolomic profiling efforts on lipid metabolites. We used single-reaction monitoring (SRM)-based targeted approaches to measure >100 lipid metabolites encompassing phospholipids, neutral lipids, sphingolipids, ether lipids, fatty acids, and eicosanoids. We also used untargeted metabolomic methods to profile the levels of an additional ~6000 ions and used XCMSOnline to identify any significantly altered metabolites. Combining targeted and untargeted metabolomic data, we found the levels of 35 lipids to be significantly changed upon KIAA1363 inhibition with JW480 in BMDMs (Figure 4C–E and Supporting Information Table 2).

While we did not observe changes in 2-acetyl MAGe levels, KIAA1363 blockade reduced MAGe levels and increased the levels of multiple LPCe (also known as lyso-PAF), LPCp, and LPAe species, suggesting that these ether lipid species may be downstream metabolic products of 2-acetyl MAGe and PAF rather than downstream of MAGe. Consistent with this premise, *d*₄-2-acetyl-MAGe isotopic incorporation studies in BMDMs revealed reduced *d*₄-incorporation into MAGe and increased *d*₄-incorporation into LPCe (lyso-PAF) and LPAe (Figure 4F). These results are in contrast to previous studies in cancer cells showing that LPCe and LPAe were downstream of MAGe metabolism. We also identified changes in multiple other ether lipid species including phosphatidylcholine-plasmalogen (PCp), phosphatidylinositol-ether (PIe), and phosphatidylglycerol-ether (PGe), likely due to network wide alterations stemming from 2-acetyl MAGe or MAGe metabolism. Interestingly, we also observed changes in additional lipid metabolism pathways including neutral lipids monoacylglycerols (MAG) and diacylglycerols (DAG), free fatty acids (FFA), *N*-acyl ethanolamines (NAEs), and phospholipids phosphatidyl ethanolamine (PE), phosphatidic acids (PA), phosphatidyl inositols (PI), lysophosphatidylcholines (LPC), lysophosphatidylethanolamine (LPE), and lysophosphatidylserines (LPS), lysophosphatidylinositols (LPI), sphingolipids ceramide, and sphingosine, indicating that KIAA1363 may directly or indirectly regulate broader metabolic pathways in lipid metabolism (Figure 4C–E).

We next wanted to determine whether these changes in specific lipid species might be driving the TNF α -lowering effects observed upon KIAA1363 inhibition. We screened representative lipid species altered by JW480 treatment for TNF α -lowering effects and found that LPCe, LPAe, and C20:4 FFA significantly reduced LPS-induced TNF α secretion in macrophages (Figure 5A). Although the specific receptor for LPCe is unknown, LPAe is known to stimulate LPA receptors,

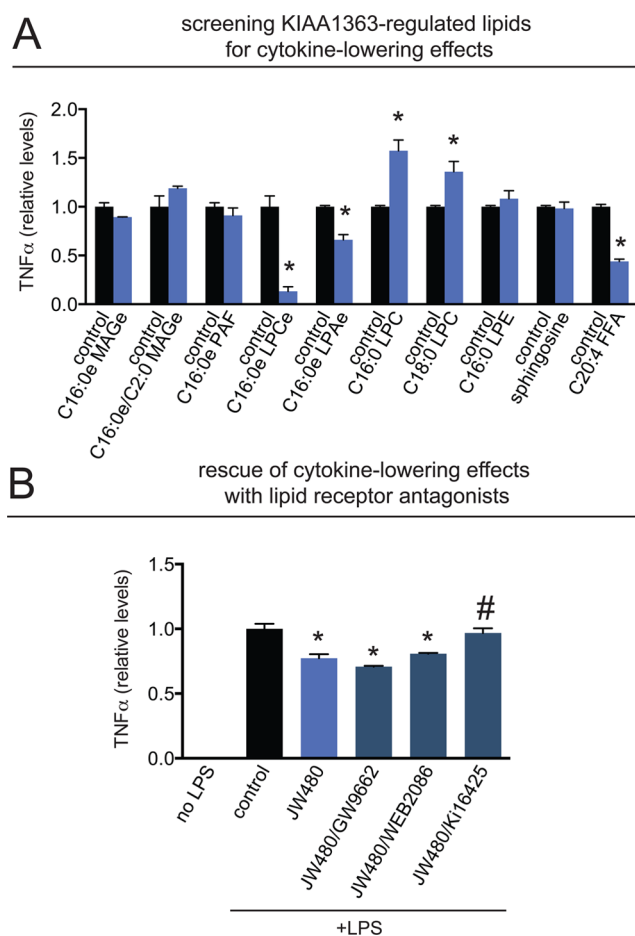


Figure 5. KIAA1363-regulated lipids possess TNF α -lowering properties. (A) The effect of KIAA1363-regulated lipids on LPS-induced TNF α release from BMDMs. BMDMs were preincubated with each lipid (10 μ M) or vehicle for 1 h before adding LPS (100 ng/mL). (B) Rescue of JW480-mediated TNF α -lowering effects by the LPA receptor antagonist Ki16425 (10 μ M) but not by the PPAR γ antagonist GW9662 (10 μ M) or the PAF receptor antagonist WEB2086 (10 μ M). Data are presented as mean \pm SEM; n = 3–4/group. Significance is presented as * p < 0.05, comparing inhibitor-treated groups to vehicle-treated, LPS-stimulated controls, or # p < 0.05 compared to JW480-treated controls.

and C20:4 FFA is an agonist of the peroxisome proliferator-activated receptor- γ (PPAR γ).^{33,34} We show that the TNF α -lowering effects of JW480 are partially reversed by treatment with an LPA receptor antagonist but not by a PPAR γ or PAF receptor antagonist, indicating that enhanced LPAe and LPA receptor signaling may be responsible for the JW480 effects (Figure 5B).

Collectively, our results show that KIAA1363 may serve as a unique metabolic node between ether lipids and other signaling lipids to drive the inflammatory response in macrophages.

Conclusions. Here, we have coupled an enzyme class-directed chemical genetics screen with ABPP platforms to identify pro-inflammatory cytokine-lowering compounds and their targets in stimulated macrophages. Using this strategy, we identified KIAA1363 and its inhibitors as a novel metabolic target that influences LPS-stimulated TNF α release. Through metabolomic profiling, we further revealed that KIAA1363 modulates inflammatory cytokine release in part through affecting LPAe and potentially other ether lipid pathways. This enzyme has also been shown to be important in driving

aggressive features of cancer cells. KIAA1363 blockade in cancer cells leads to a reduction in the levels of LPAe, which leads to reduced motility and tumor growth. In cancer cells, LPAe is downstream of the KIAA1363 product MAGE, whereas our studies in BMDMs suggest that LPAe is downstream of LPCe, a metabolite arising from PAF hydrolysis.³¹ Thus, our data indicate that the KIAA1363–ether lipid pathway may be wired differently in these two different contexts. Holly et al. also discovered that KIAA1363 regulates platelet aggregation, thrombus growth, RAP1 and PKC activation, ether lipid metabolism, and fibrinogen binding to platelets and megakaryocytes.²⁸ Thus, KIAA1363 inhibitors potentially possess multiple biological activities through manipulating ether lipid signaling pathways and show multiple potential therapeutic avenues.

Our study underscores the utility of combining chemical genetics with chemical systems biology platforms such as ABPP and functional metabolomic profiling toward identifying and characterizing anti-inflammatory small molecules and their targets.

METHODS

Materials. The THP1 cell line was purchased from ATCC. Mouse colony stimulating factor (M-CSF) was purchased from Cell Signaling Technologies. *d*₄-PAF was purchased from Cayman Chemical. Internal standards and metabolite standards were purchased from Sigma, Cayman Chemicals, or Avanti Polar Lipids. The carbamate, phosphonate, and triazole urea inhibitors were obtained from Professor Benjamin Cravatt at The Scripps Research Institute and Professor John Casida at the University of California, Berkeley, or were synthesized. The synthesis and characterization of the materials obtained from the Cravatt and Casida laboratories are described previously.^{17,18,21–23} Synthetic methods and characterization of lead compounds that were synthesized in our lab are described in Supporting Information Methods. The KIAA1363 inhibitor JW480 was purchased from Cayman Chemicals. FP-biotin was synthesized as previously described.³⁵

Cell Culture Conditions. THP1 cells were cultured in RPMI supplemented with 10% FBS, L-glutamine, and β -mercaptoethanol and maintained in a humidified incubator at 37 °C in an atmosphere of 5% CO₂. BMDMs were cultured in DMEM supplemented with 10% FBS, L-glutamine, and 20 ng/mL M-CSF and maintained in a humidified incubator at 37 °C in an atmosphere of 8% CO₂.

Isolation of Murine Bone Marrow-Derived Macrophages. Bone marrow was isolated from the femurs and tibias of male C57BL/6 mice (10–12 week) using a mortar and pestle in complete media containing DMEM supplemented with 10% FBS, L-glutamine, and 20 ng/mL M-CSF. Particulate matter was removed by slow-speed centrifugation. Bone marrow cells were then pelleted by centrifugation, resuspended, and plated in complete media on nontreated plastic. Medium was replaced every 2–3 days. On day 7, adherent cells were washed and incubated at 4 °C for 20 min. Cells were gently scraped, isolated by centrifugation, counted, and plated for experiments.

Cytokine Quantification. THP-1 (10⁶/well) or BMDMs (100 000–200 000 cells/well in 24-well plates) were plated. Cells were switched to serum-free media, and inhibitors, lipids, and/or antagonists were added for 1 h. After stimulation with 100 ng/mL LPS for 6 h, media was collected, and TNF α levels were quantified by ELISA per the manufacturer's instructions (Qiagen).

Survival Assays. Cell survival analysis was performed using the Hoechst 33342 nuclear stain (Invitrogen). Briefly, 20 000 cells were seeded into 96-well plates in a volume of 100 μ L for 0, 24, and 48 h in the presence of inhibitors in serum-free DMEM. Cells were washed, fixed, and stained according to the manufacturer's protocol. Plates were scanned using the fluorescence excitation/emission wavelengths for Hoechst 33342 (350 and 461 nm, respectively).

***d*₄-2-Acetyl MAGE Synthesis.** *d*₄-C16:0 2-acetyl MAGE was prepared from [*d*₄-C16:0e] PAF by incubation with 20 units phospholipase C from *Bacillus cereus* (Sigma-Aldrich) in PBS for 45 min at RT as described previously.³² Completion of the reaction was confirmed by LC–MS. The product was extracted in 2:1 chloroform/methanol, and the organic layer was dried under N₂ and resuspended in 2:1 chloroform/methanol to the desired concentration.

KIAA1363 Activity Assays. BMDMs were treated with JW480 (5 μ M in DMSO) or DMSO for 4 h. BMDM cell lysates (25 μ g) were incubated with *d*₄-2-acetyl MAGE (100 μ M final concentration) for 30 min at RT in PBS (200 μ L total volume). To quench the reaction, 1:1 ethyl acetate/hexanes was added (600 μ L), followed by vortexing and addition of internal standards. After centrifugation, the organic layer was removed for analysis of *d*₄-MAGE formation by LC–MS.

Lipidomic Profiling of Macrophages. BMDMs were plated (3 \times 10⁶ cell/well of 6-well plate) and allowed to adhere overnight. Cells were washed with PBS, switched to serum-free media containing JW480 (5 μ M) or DMSO control for 1 h, and then stimulated with LPS (100 ng/mL) for 6 h. Cells were washed with PBS, harvested by scraping, and isolated by centrifugation. Cell pellets were flash-frozen and stored at –80° until extraction.

Nonpolar lipid metabolites were extracted and analyzed by targeted and untargeted metabolomic methods using previously described procedures.^{36,37} Briefly, lipid metabolites were extracted in a 2:1:1 chloroform/methanol/PBS with addition of internal standards C12:0 dodecylglycerol (10 nmol) and pentadecanoic acid (10 nmol). Organic and aqueous layers were separated by centrifugation at 1000g for 5 min, and the organic layer was collected. The aqueous layer was acidified by the addition of 0.1% formic acid followed by the addition of 2 mL chloroform, vortexing, and centrifugation. The organic layers were combined, dried under N₂, and resuspended in 120 μ L of chloroform. An aliquot (10 μ L) was analyzed by single-reaction monitoring (SRM)-based LC–MS/MS. LC separation was achieved with a Luna reverse-phase C5 column (Phenomenex). Mobile phase A was composed of 95:5 water/methanol, and mobile phase B consisted of 60:35:5 isopropanol/methanol/water. Solvent modifiers 0.1% formic acid with 5 mM ammonium formate and 0.1% ammonium hydroxide were used to assist ion formation and to improve the LC resolution in both positive and negative ionization modes, respectively. The flow rate for each run started at 0.1 mL/min for 5 min to alleviate backpressure associated with injecting chloroform. The gradient started at 0% B and increased linearly to 100% B over the course of 45 min with a flow rate of 0.4 mL/min, followed by an isocratic gradient of 100% B for 17 min at 0.5 mL/min before equilibrating for 8 min at 0% B with a flow rate of 0.5 mL/min.

MS analysis was performed with an electrospray ionization source (ESI) on an Agilent 6430 QQQ LC–MS/MS. Lipid metabolites were quantified by SRM of the precursor to product ion transition at associated collision energies as previously described.^{36,37} Quantification was achieved by integrating the area under the peak and expressed as a percent of control after normalizing to the internal standard.

ABPP Analysis of Macrophages. For gel-based ABPP experiments, BMDMs were treated with inhibitor (5 μ M in DMSO) or DMSO control for 4 h, harvested by scraping, and pelleted by centrifugation. BMDM cell lysate proteomes (50 μ g) were labeled with FP-rhodamine (2 μ M) for 30 min at RT, quenched with 4 \times SDS/PAGE loading buffer, heated at 95 °C for 5 min, and separated by 10% SDS/PAGE as previously described. Gels were scanned using a Typhoon flatbed fluorescence scanner (GE Healthcare).

ABPP-MudPIT analysis was performed using previously established methods. BMDMs were treated with inhibitor (5 μ M in DMSO) or DMSO control for 4 h, harvested by scraping, and pelleted by centrifugation. Briefly, BMDM proteome (1 mg) was labeled with FP-biotin (5 μ M) in 1 mL PBS for 1 h, solubilized in 1% Triton X-100 for 1 h, and denatured. Labeled enzymes were enriched using avidin beads, reduced, alkylated, and trypsinized as previously described.³⁸ Tryptic peptides were loaded on to a strong cation exchange/reverse-phase capillary column and analyzed by two-dimensional LC–LC–MS/MS, also known as multidimensional protein identification

technology (MudPIT), as previously described.³⁸ Resulting MS² datafiles were then analyzed by Integrated Proteomics Pipeline.

***d*₄-2-Acetyl MAGE Isotopic Labeling.** BMDMs (2×10^6 cells) were plated and allowed to adhere overnight. Cells were pretreated in serum-free media with JW480 (5 μ M in DMSO) or DMSO control for 1 h and then stimulated with LPS (100 ng/mL) and *d*₄-2-acetyl MAGE (10 μ M) for 15 min. Cells were washed, scraped on ice, and immediately extracted in 2:1 chloroform/methanol as described above. Isotopic incorporation was detected and quantified using targeted LC–MS using SRM transitions based on previously derived optimized transitions of nonisotopic standards.

■ ASSOCIATED CONTENT

■ Supporting Information

Figure 1: MAGL inhibition does not alter LPS-induced TNF α levels; compound characterization. This material is available free of charge via the Internet at <http://pubs.acs.org>.

■ AUTHOR INFORMATION

Corresponding Author

*E-mail: dnomura@berkeley.edu.

Notes

The authors declare no competing financial interest.

■ ACKNOWLEDGMENTS

We thank Dr. K. Collins of the University of California, Berkeley, for use of her Typhoon flatbed scanner. This work was supported by the Searle Foundation, the Hellman Fellows program, a gift from M. Winkler and the Winkler Family Foundation, startup funds from the University of California, Berkeley College of Natural Resources, and the National Institutes of Health (R01CA172667). The 900 MHz NMR spectrometer was generously funded by National Institutes of Health grant GM68933.

■ REFERENCES

- (1) Donath, M. Y. (2014) Targeting inflammation in the treatment of type 2 diabetes: time to start. *Nat. Rev. Drug Discovery* 13, 465–476.
- (2) Glass, C. K., Saijo, K., Winner, B., Marchetto, M. C., and Gage, F. H. (2010) Mechanisms underlying inflammation in neurodegeneration. *Cell* 140, 918–934.
- (3) Grivennikov, S. I., Greten, F. R., and Karin, M. (2010) Immunity, inflammation, and cancer. *Cell* 140, 883–899.
- (4) Nathan, C., and Ding, A. (2010) Nonresolving inflammation. *Cell* 140, 871–882.
- (5) Wymann, M. P., and Schneider, R. (2008) Lipid signalling in disease. *Nat. Rev. Mol. Cell Biol.* 9, 162–176.
- (6) Serhan, C. N., Chiang, N., and Van Dyke, T. E. (2008) Resolving inflammation: dual anti-inflammatory and pro-resolution lipid mediators. *Nat. Rev. Immunol.* 8, 349–361.
- (7) Gilroy, D. W., Lawrence, T., Perretti, M., and Rossi, A. G. (2004) Inflammatory resolution: new opportunities for drug discovery. *Nat. Rev. Drug Discovery* 3, 401–416.
- (8) Kohnz, R. A., and Nomura, D. K. (2014) Chemical approaches to therapeutically target the metabolism and signaling of the endocannabinoid 2-AG and eicosanoids. *Chem. Soc. Rev.* 43, 6859–6869.
- (9) Dinarello, C. A. (2010) Anti-inflammatory agents: present and future. *Cell* 140, 935–950.
- (10) Asanuma, M., and Miyazaki, I. (2008) Nonsteroidal anti-inflammatory drugs in experimental parkinsonian models and Parkinson's disease. *Curr. Pharm. Des.* 14, 1428–1434.
- (11) Luo, P., and Wang, M. H. (2011) Eicosanoids, beta-cell function, and diabetes. *Prostaglandins Other Lipid Mediators* 95, 1–10.
- (12) Wang, D., and Dubois, R. N. (2010) Eicosanoids and cancer. *Nat. Rev. Cancer* 10, 181–193.
- (13) Mitchell, J. A., and Warner, T. D. (2006) COX isoforms in the cardiovascular system: understanding the activities of non-steroidal anti-inflammatory drugs. *Nat. Rev. Drug Discovery* 5, 75–86.
- (14) Cong, F., Cheung, A. K., and Huang, S. M. (2011) Chemical genetics-based target identification in drug discovery. *Annu. Rev. Pharmacol. Toxicol.* 52, 57–78.
- (15) Long, J. Z., and Cravatt, B. F. (2011) The metabolic serine hydrolases and their functions in mammalian physiology and disease. *Chem. Rev.* 111, 6022–6063.
- (16) Bachovchin, D. A., and Cravatt, B. F. (2012) The pharmacological landscape and therapeutic potential of serine hydrolases. *Nat. Rev. Drug Discovery* 11, 52–68.
- (17) Adibekian, A., Martin, B. R., Wang, C., Hsu, K. L., Bachovchin, D. A., Niessen, S., Hoover, H., and Cravatt, B. F. (2011) Click-generated triazole ureas as ultrapotent *in vivo*-active serine hydrolase inhibitors. *Nat. Chem. Biol.* 7, 469–478.
- (18) Bachovchin, D. A., Ji, T., Li, W., Simon, G. M., Blankman, J. L., Adibekian, A., Hoover, H., Niessen, S., and Cravatt, B. F. (2010) Superfamily-wide portrait of serine hydrolase inhibition achieved by library-versus-library screening. *Proc. Natl. Acad. Sci. U.S.A.* 107, 20941–20946.
- (19) Chang, J. W., Nomura, D. K., and Cravatt, B. F. (2011) A potent and selective inhibitor of KIAA1363/AADACL1 that impairs prostate cancer pathogenesis. *Chem. Biol.* 18, 476–484.
- (20) Long, J. Z., Nomura, D. K., Vann, R. E., Walentiny, D. M., Booker, L., Jin, X., Burston, J. J., Sim-Selley, L. J., Lichtman, A. H., Wiley, J. L., and Cravatt, B. F. (2009) Dual blockade of FAAH and MAGL identifies behavioral processes regulated by endocannabinoid crosstalk *in vivo*. *Proc. Natl. Acad. Sci. U.S.A.* 106, 20270–20275.
- (21) Nomura, D. K., Hudak, C. S., Ward, A. M., Burston, J. J., Issa, R. S., Fisher, K. J., Abood, M. E., Wiley, J. L., Lichtman, A. H., and Casida, J. E. (2008) Monoacylglycerol lipase regulates 2-arachidonoylglycerol action and arachidonic acid levels. *Bioorg. Med. Chem. Lett.* 18, 5875–5878.
- (22) Nomura, D. K., Durkin, K. A., Chiang, K. P., Quistad, G. B., Cravatt, B. F., and Casida, J. E. (2006) Serine hydrolase KIAA1363: toxicological and structural features with emphasis on organophosphate interactions. *Chem. Res. Toxicol.* 19, 1142–1150.
- (23) Nagano, J. M., Hsu, K. L., Whitby, L. R., Niphakis, M. J., Speers, A. E., Brown, S. J., Spicer, T., Fernandez-Vega, V., Ferguson, J., Hodder, P., Srinivasan, P., Gonzalez, T. D., Rosen, H., Bahnson, B. J., and Cravatt, B. F. (2013) Selective inhibitors and tailored activity probes for lipoprotein-associated phospholipase A₂. *Bioorg. Med. Chem. Lett.* 23, 839–843.
- (24) Hunerdosse, D., and Nomura, D. K. (2014) Activity-based proteomic and metabolomic approaches for understanding metabolism. *Curr. Opin. Biotechnol.* 28, 116–126.
- (25) Moellerling, R. E., and Cravatt, B. F. (2012) How chemo-proteomics can enable drug discovery and development. *Chem. Biol.* 19, 11–22.
- (26) Nomura, D. K., Dix, M. M., and Cravatt, B. F. (2010) Activity-based protein profiling for biochemical pathway discovery in cancer. *Nat. Rev. Cancer* 10, 630–638.
- (27) Dominguez, E., Galmozzi, A., Chang, J. W., Hsu, K. L., Pawlak, J., Li, W., Godio, C., Thomas, J., Partida, D., Niessen, S., O'Brien, P. E., Russell, A. P., Watt, M. J., Nomura, D. K., Cravatt, B. F., and Saez, E. (2014) Integrated phenotypic and activity-based profiling links Ces3 to obesity and diabetes. *Nat. Chem. Biol.* 10, 113–121.
- (28) Holly, S. P., Chang, J. W., Li, W. W., Niessen, S., Phillips, R. M., Piatt, R., Black, J. L., Smith, M. C., Boulaftali, Y., Weyrich, A. S., Bergmeier, W., Cravatt, B. F., and Parise, L. V. (2013) Chemo-proteomic discovery of AADACL1 as a regulator of human platelet activation. *Chem. Biol.* 20, 1125–1134.
- (29) Osuga, J., Ishibashi, S., Oka, T., Yagyu, H., Tozawa, R., Fujimoto, A., Shionoiri, F., Yahagi, N., Kraemer, F. B., Tsutsumi, O., and Yamada, N. (2000) Targeted disruption of hormone-sensitive lipase results in male sterility and adipocyte hypertrophy, but not in obesity. *Proc. Natl. Acad. Sci. U.S.A.* 97, 787–792.

- (30) Lotti, M., and Moretto, A. (2005) Organophosphate-induced delayed polyneuropathy. *Toxicol. Rev.* 24, 37–49.
- (31) Chiang, K. P., Niessen, S., Saghatelian, A., and Cravatt, B. F. (2006) An enzyme that regulates ether lipid signaling pathways in cancer annotated by multidimensional profiling. *Chem. Biol.* 13, 1041–1050.
- (32) Nomura, D. K., Fujioka, K., Issa, R. S., Ward, A. M., Cravatt, B. F., and Casida, J. E. (2008) Dual roles of brain serine hydrolase KIAA1363 in ether lipid metabolism and organophosphate detoxification. *Toxicol. Appl. Pharmacol.* 228, 42–48.
- (33) Liu, S., Murph, M., Panupinthu, N., and Mills, G. B. (2009) ATX–LPA receptor axis in inflammation and cancer. *Cell Cycle* 8, 3695–3701.
- (34) Berger, J., and Moller, D. E. (2002) The mechanisms of action of PPARs. *Annu. Rev. Med.* 53, 409–435.
- (35) Liu, Y., Patricelli, M. P., and Cravatt, B. F. (1999) Activity-based protein profiling: the serine hydrolases. *Proc. Natl. Acad. Sci. U.S.A.* 96, 14694–14699.
- (36) Benjamin, D. I., Cozzo, A., Ji, X., Roberts, L. S., Louie, S. M., Mulvihill, M. M., Luo, K., and Nomura, D. K. (2013) Ether lipid generating enzyme AGPS alters the balance of structural and signaling lipids to fuel cancer pathogenicity. *Proc. Natl. Acad. Sci. U.S.A.* 110, 14912–14917.
- (37) Mulvihill, M. M., Benjamin, D. I., Ji, X., Le Scolan, E., Louie, S. M., Shieh, A., Green, M., Narasimhalu, T., Morris, P. J., Luo, K., and Nomura, D. K. (2014) Metabolic profiling reveals PAFAH1B3 as a critical driver of breast cancer pathogenicity. *Chem. Biol.* 21, 831–840.
- (38) Nomura, D. K., Long, J. Z., Niessen, S., Hoover, H. S., Ng, S. W., and Cravatt, B. F. (2010) Monoacylglycerol lipase regulates a fatty acid network that promotes cancer pathogenesis. *Cell* 140, 49–61.